Communication

Endosomal Escape and Delivery of CRISPR/Cas9 Genome Editing Machinery Enabled by Nanoscale Zeolitic Imidazolate Framework

Shahad K. Alsaiari, Sachin Patil, Mram Alyami, Kholod Alamoudi,
fajr Aleisa, Jasmeen Merzaban, Mo Li, and Niveen M Khashab

Just Accepted

Endosomal Escape and Delivery of CRISPR/Cas9 Genome Editing Machinery Enabled by Nanoscale Zeolitic Imidazolate Framework

Shahad K. Alsaiari,[†] Sachin Patil,[†] Mram Alyami,[†] Kholod O. Alamoudi,[†] Fajr A. Aleisa,[§] Jasmeen S. Merzaban,[§] Mo Li,[‡] Niveen M. Khashab[*,†]

[†] Smart Hybrid Materials (SHMs) Laboratory, Advanced Membranes and Porous Materials Center, King Abdullah University of Science and Technology (KAUST), Thuwal 23955-6900, Saudi Arabia.

[§] Cell Migration and Signaling Laboratory, Division of Biological and Environmental Science and Engineering, King Abdullah University of Science and Technology (KAUST), Thuwal 23955-6900, Saudi Arabia

[‡] Stem Cell and Regeneration Laboratory, Division of Biological and Environmental Science and Engineering, King Abdullah University of Science and Technology (KAUST), Thuwal 23955-6900, Saudi Arabia.

Supporting Information

ABSTRACT: CRISPR/Cas9 is a combined protein (Cas9) and an engineered single guide RNA (sgRNA) genome editing platform that offers revolutionary solutions to genetic diseases. It has, however, a double delivery problem owning to the large protein size and the highly charged RNA component. In this work, we report the first example of CRISPR/Cas9 encapsulated by nanoscale zeolitic imidazole frameworks (ZIFs) with a loading efficiency of 17% and enhanced endosomal escape promoted by the protonated imidazole moieties. The gene editing potential of CRISPR/Cas9 encapsulated by ZIF-8 (CC-ZIFs) is further verified by knocking down the gene expression of green fluorescent protein by 37% over 4 days. The nanoscale CC-ZIFs are biocompatible and easily scaled-up offering excellent loading capacity and controlled co-delivery of intact Cas9 protein and sgRNA.

CRISPR/Cas9, the clustered regularly interspaced short palindromic repeat (CRISPR) associated proteins 9 (Cas9) technology, is a recently developed site-specific gene editing platform that uses single guide RNA (sgRNA) for site recognition.[1-3] The protein complex targets the DNA sequence of interest via the sgRNA. DNA strands complementary to the sgRNA are cleaved by Cas9 protein. The break is then repaired by non-homologous end-joining (NHEJ) or homology-directed repair (HR). Recently, several studies have reported the applicability of CRISPR/Cas9 technology as a powerful therapeutic strategy against viruses,[4] bacteria[5] and cancer.[6] However, for all the enthusiastic upside surrounding the prospects of RNA-based therapeutics, there continues to be an equal and opposite downside that started many years ago, namely the delivery problem. As these therapeutic platforms are usually taken up by endocytosis, they remain trapped inside the endosome, behind the lipid bilayer, and as such are outside of the cytoplasm and the nucleus.[7] With a current endosomal escape not exceeding 0.01%, devising new approaches to get such therapeutic platforms into the nucleus and overcome the endosomal escape abyss is the key technological problem to solve before investigating the full potential of such revolutionary therapeutic technologies.

CRISPR has a double delivery problem because two macromolecules are required for a functional therapeutic system: one, a large catalytic Cas9 recombinase that is ~160 kDa and two, a ~150 nucleotide tracer/sg RNA.[1-2] Although these components will invariably get somewhat smaller by using a low molecular

Scheme 1. Preparation, cytosolyic delivery and gene editing efficiency of CC-ZIFs. (a) Encapsulating the negatively charged Cas9/sgRNA within positively charged ZIF-8 to form CC-ZIFs. (b) Endosomal escape of CC-ZIFs. (c) CLSM images of cells before and after treatment with CC-ZIFs.
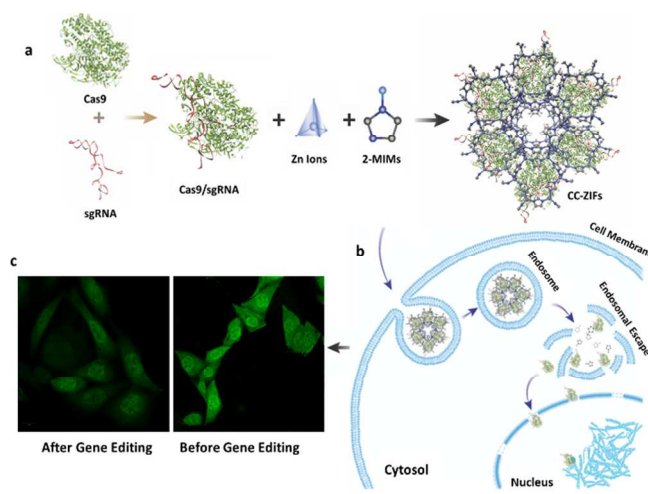
weight CRISPR recombinase and/or shorter sgRNAs, from a delivery perspective, these are still very large and charged problematic macromolecules. Most of CRISPR/Cas9 studies so far have depended on viral or physical delivery; however, the immunogenicity complications of the viral vectors and the difficulty of translating physical delivery protocols in vivo have empowered the need to accomplish such delivery through synthetic nanoparticles.[8-9] Cationic lipid nanoparticles,[10] gold nanoparticles[11] and DNA nanoclews[12] have been successfully employed for delivery of Cas9. More recently zwitterionic amino lipids were used as delivery vehicles,

however the co-delivery was of Cas9 mRNA and not the actual protein.[13]

Zeolitic imidazolate framework-8 (ZIF-8) are a subclass of metal–organic frameworks formed by coordination between Zn^{2+} ions and 2-methylimidazole.[14-16] They have good biocompatibility[17, 18] and remarkably tunable pore openings[19] for a wide range of guest molecules. Recently, ZIFs have been successfully used for drug delivery [20], ATP imaging [21] and biomimetic mineralization or sheltering of biomacromolecules.[22, 23] Moreover, the imidazole linkers are known to have excellent pH-buffering capacity, which is presumed to confer enhanced ability to escape the endocytic pathway.[24, 25] Herein, we report the first example of nanoscale ZIF-8 co-encapsulating Cas9 protein and sgRNA (CC-ZIFs) with a remarkable loading efficiency of 17% and enhanced endosomal escape leading to 37% reduction in gene expression over four days (Scheme 1). This work opens up new possibilities for exceptionally improved genetic materials delivery enabled by precisely engineered biocompatible smart coordination frameworks.
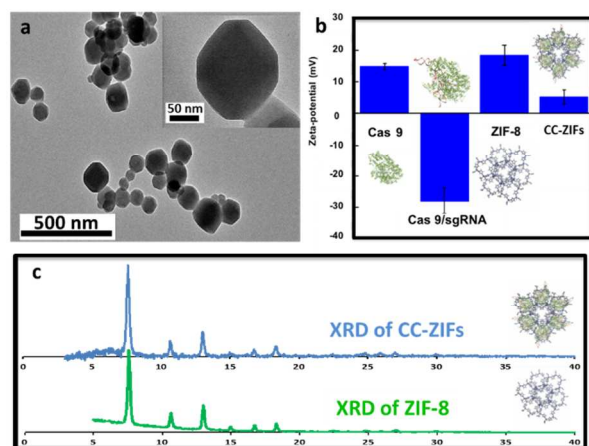

Figure 1. Characterization of CC-ZIFs. (a) TEM micrographs of CC-ZIFs at different scales. (b) Zeta potential of free Cas9, Cas9/sgRNA complex, ZIF-8 and CC-ZIFs. Bars represent mean± SD (n=3). (c) PXRD of ZIF-8 (green) and CC-ZIFs (blue).

CC-ZIFs were prepared by first mixing Cas9 and sgRNA at a molar ratio of 1:1 in a phosphate buffer saline (PBS) for 5 minutes followed by addition of 2-methylimidazole solution (0.9 mL, 5 M, pH 7). An aqueous solution of zinc nitrate (0.1 mL, 0.5 M) was then slowly added at room temperature under mechanical agitation for 20 minutes after which the clear solution turned opaque (Scheme 1a). The resulting CC-ZIFs were then collected by centrifugation after washing with DI water (3 cycles) to remove all residues. The truncated ZIF-8 cubic crystals were first characterized by tunneling electron microscopy (TEM) showing an average size of 100 nm that is ideal for intracellular delivery (Figure 1a). The average size was confirmed by dynamic light scattering analysis (DLS) at neutral conditions (Figure S1). Measuring zeta potential showed that the positively charged Cas9 (+15 mV ± 1) became negatively charged upon the addition of sgRNA (-28 mV± 4). After metal-coordination sheltering of the complex and formation of CC-ZIFs the zeta potential measured at + 5 mV ± 2, which is less positive than the native ZIF-8 (+17 mV ±1) (Figure 1b). Furthermore, powder X-

ray diffraction (PXRD) graphs showed that the Cas9/sgRNA@ZIF-8 has the same crystal structure as that of the pure ZIF-8 (Figure 1c).
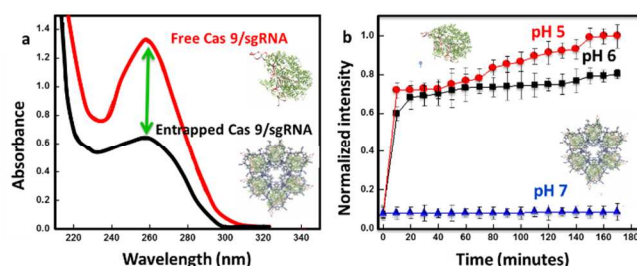

Figure 2. CRISPR/Cas9 loading and release. (a) UV-VIS spectra of Alexa fluora (AF) labeled CC-ZIFs compared to free AF-Cas9/sgRNA complex. (b) pH dependent release of AF-Cas9/sgRNA from CC-ZIFs.

CRISPR/Cas9 loading efficiency and pH responsive release were tested by labeling Cas9 with Alexa fluor 647 (AF). The red fluorescence of AF-Cas9 in the supernatant decreased drastically after the de novo encapsulation within ZIF-8 (Figure S2a). The loading capacity was calculated to be 1.2 wt % with efficiency of 17 % (Figure 2a), which is consistent with the loading capacity of previously reported MOF based delivery systems.[23] To evaluate the stability of AF-CC-ZIFs under physiological (pH 7.4) and acidic (pH 5 and 6) conditions, they were dispersed in PBS solution. DLS analysis showed a stable structure at neutral conditions that starts degrading directly at acidic pH (Figure S1). CC-ZIFs completely decomposed after 6 hours at pH 5.5 (Figure S1). The release of AF-Cas9 was monitored by fluorescence spectroscopy (Figure 2b, Figure S2b). Under physiological conditions less than 3 % of AF-Cas9 was released while 60 % and 70 % were released in 10 minutes at pH 6 and 5, respectively. The maximum release of AF-Cas9 was observed at pH 5 within 3 hours, exploiting the selectivity of CC-ZIFs release under acidic conditions. The release mechanism of CC-ZIFs is superior to reported protein delivery systems, such as Au NPs and DNA cages, in a sense that it is associated with a complete and safe dissolution of ZIF-8 at low pH without leaving residue nanoparticles or denaturation of DNA strands.

Biocompatibility of CC-ZIFs was tested at different concentrations by incubation with Chinese hamster ovary (CHO) cells for 12 hours. CHO cells were washed and evaluated by the cell counting kit-8 (CCK-8). Compared to native CHO group, no measurable impact was seen at concentrations below 200 µg mL^{-1}, whereas higher concentrations (≥ 200 µg mL^{-1}) led to the increased cytotoxicity in both ZIF-8 and CC-ZIFs (Figure S3a, S3b). Based on the CCK-8 results, we examined the toxicity of 250 and 100 µg mL^{-1} of ZIF-8 and CC-ZIFs by live-dead cell staining using flow cytometry (Figure S3c–S3f). No significant cell death was observed even after 12 hours of transfection at a concentration of 100 µg mL^{-1}. The lethal dose (LD50) of ZIFs and CC-ZIFs was determined to be 400 and 420 µg mL^{-1}, respectively (Figure S3g). Based on these results, a concentration of 100 µg mL^{-1} of CC-ZIFs was used in all subsequent experiments. We examined the capability of ZIF-8 to deliver AF-Cas9/sgRNA by flow cytometry and confocal laser scanning microscopy (CLSM). The intensity of red AF 647

increased with time suggesting the delivery of more Cas9/sgRNA into the cytoplasm (Figure S4a). CLSM images showed that AF-Cas9/sgRNA internalized in the nucleus after 3 hours (Figure S4b). In 6 hours, many AF-Cas9/sgRNA were seen in nuclei, elucidating the increase in the AF-Cas9 signal in the flow cytometry data (Figure S4b). As a control, free AF-Cas9/sgRNA was not delivered into cells as the signal of AF-Cas9/sgRNA was not detected by flow cytometry (Figure S4c) or CLSM (Figure S4d) over the same period of time.
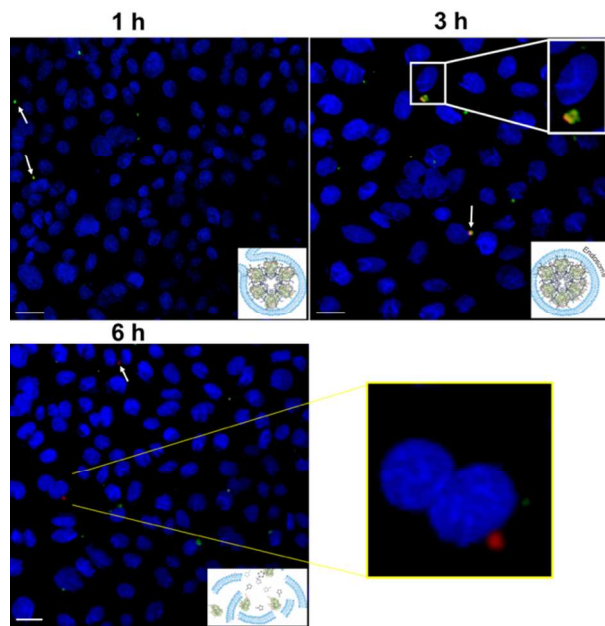

Figure 3. CLSM images (40x) of CHO cells after incubation with AF-CC-ZIFs (red) for 1, 3 and 6 hours. Lysotracker Green (green) was used to stain the acidic organelles (endosomes). The merged images are used to confirm that AF-Cas9/sgRNA is released and delivered into the nucleus within 6 hours of uptake. Scar bar: 20 μm.

To assess the endosomal escape associated with CC-ZIFs, CHO cells were first transfected with particles at different time points (1, 3 and 6 hours), to examine the cellular transfection efficiency. The endosomal escape of CC-ZIFs is mediated by the protonation of the imidazole ring,[24] which is followed by the release of Cas9/sgRNA to the cytoplasm. AF-Cas9/sgRNA localized inside endosomes within 1 hour of transfection, which was observed in yellow merged color (Figure 3). In contrast, 3 and 6 hours post transfection showed complete separation between red Cas9 and green endosomes indicating the release of Cas9/sgRNA from endosomes. Images at 20x were also obtained to show that many cas9 were released form ZIF-8 upon their protonation (Figure S6). We then compared our system's ability to escape endosomal encapsulation to a cationic liposome based delivery system.[10] The obtained results with the same cell line over the same period of time showed a complete localization of the liposomes within endosomes (Figure S5).

To demonstrate the efficiency of gene knockdown by CC-ZIFs, we used sgRNA to target the coding region of the enhanced green fluorescent protein (EGFP) in CHO cells. Targeting the coding region will result in shifting the reading frame and consequently preventing proper EGFP expression.

EGFP transfected CHO cells were treated with free Cas9/sgRNA, ZIF-8 and CC-ZIFs for 2 days. We also investigated whether incubating cells for more than 2 days would change EGFP gene expression so cells were incubated for 4 days after treatment. The fluorescence and expression of EGFP were determined by CLSM, flow cytometry and quantitative real-time polymerase chain reaction (qRT-PCR). Measuring the EGFP fluorescence using flow cytometry demonstrates that CC-ZIFs reduced the fluorescence of EGFP by 31 % when incubated for 2 days and 37 % when incubated for 4 days (Figure 4a, Figure 4c).
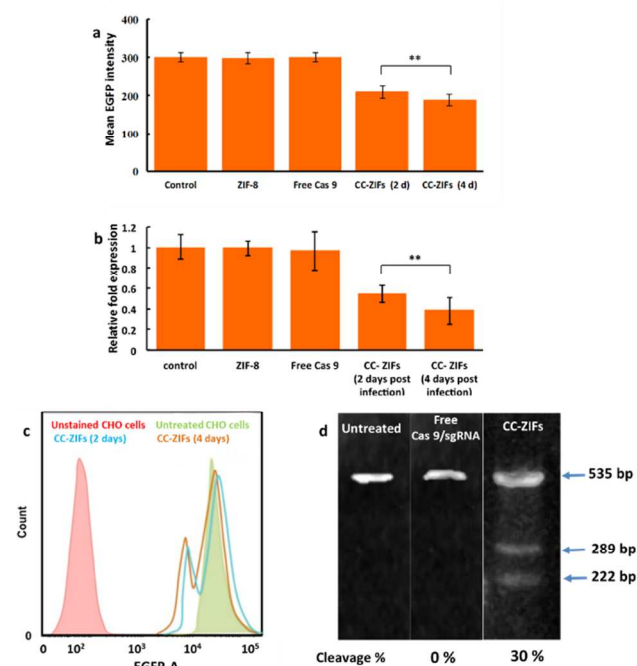

Figure 4. Genome editing by CC-ZIFs. (a, c) Flow cytometry analysis of EGFP expression at day 2 and 4 at concentration of 100 μg mL^{-1} (encapsulated Cas9/sgRNA 240 nM). (b) quantitation of EGFP expression by qPCR at concentration of 240 nM for 2 and 4 days. Statistical analysis was determined using unpaired t-test (***P< 0.001, **P<0.01, *P<0.1). (d) Surveyor assay for indel frequency analysis of EGFP transfected CHO cells incubated with free Cas9/sgRNA and CC-ZIFs.

No effect was seen on the EGFP fluorescence when cells were treated with free Cas9/sgRNA and ZIF-8, demonstrating the importance of ZIF-8 in the delivery of Cas9/sgRNA. CLSM images also confirmed the quenching of the EGFP fluorescence when ZIF-8 was used to deliver Cas9/sgRNA (Figure S7). These results were refined by quantifying the mRNA levels of EGFP in free Cas9/sgRNA, ZIF-8 and CC-ZIFs treated CHO cells by qRT-PCR. Our results demonstrate that CC-ZIFs effectively delivered Cas9/sgRNA and the sgRNA targeted the EGFP coding region causing 2-fold repression of EGFP gene when cells were incubated for 2 days (Figure 4b). Incubating cells for 4 days post treatment resulted in decreasing the fluorescence of EGFP by 37 % and reduction of the level of EGFP gene expression by 3-folds. Free Cas9/sgRNA and ZIF-8 had no effect on the expression of EGFP (Figure 4b). The efficiency of gene knockdown by CC-ZIFs was compared to the Lipofectamine CRISPRMAX Cas9. The concentration

of Cas9/sgRNA used in lipofectamine was 240 nM. The Lipofectamine CRISPRMAX Cas9 resulted in only1-fold and 1.5-fold repression of EGFP gene in 2 and 4 days after treatment, respectively (Figure S8). Surveyor assay revealed mutation frequencies of 0 % and 30 % for cells treated with free Cas9/sgRNA and CC-ZIFs for 2 days (Figure 4c), respectively, closely paralleling the results of flow cytometry, CLSM and qRT-PCR.

In conclusion, we demonstrate the first example of CRISPR/ Cas9 delivery by metal-coordination frameworks. ZIF-8 can successfully shelter both the large Cas9 protein and the negatively charged sgRNA with a high loading capacity of 1.2 wt%. The protonation of the imidazole based framework at endosomal pH promotes fast endosomal escape and enhanced nuclei delivery, which is paramount for genetic transfection. This system provides a one-step route for the creation of effective and transient gene editing technology.

ASSOCIATED CONTENT

Supporting Information

The Supporting Information is available free of charge on the ACS Publications website.
Characterization data (DLS, TEM and fluorescence spectroscopy), Cytotoxicity and uptake data.

AUTHOR INFORMATION

Corresponding Author

 * Niveen.khashab@kaust.edu.sa

REFERENCES

1. Jinek, M.; Chylinski, K.; Fonfara, I.; Hauer, M.; Doudna, J. A.; Charpentier, E., A programmable dual-RNA-guided DNA endonuclease in adaptive bacterial immunity. *Science* **2012,** *337* (6096), 816-21.

2. Cong, L.; Ran, F. A.; Cox, D.; Lin, S. L.; Barretto, R.; Habib, N.; Hsu, P. D.; Wu, X. B.; Jiang, W. Y.; Marraffini, L. A.; Zhang, F., Multiplex Genome Engineering Using CRISPR/Cas Systems. *Science* **2013,** *339* (6121), 819-823.

3. Mali, P.; Yang, L.; Esvelt, K. M.; Aach, J.; Guell, M.; DiCarlo, J. E.; Norville, J. E.; Church, G. M., RNA-guided human genome engineering via Cas9. *Science* **2013,** *339* (6121), 823-6.

4. Liao, H. K.; Gu, Y.; Diaz, A.; Marlett, J.; Takahashi, Y.; Li, M.; Suzuki, K.; Xu, R.; Hishida, T.; Chang, C. J.; Esteban, C. R.; Young, J.; Belmonte, J. C. I., Use of the CRISPR/Cas9 system as an intracellular defense against HIV-1 infection in human cells. *Nature Communications* **2015,** *6*.

5. Choudhary, E.; Thakur, P.; Pareek, M.; Agarwal, N., Gene silencing by CRISPR interference in mycobacteria. *Nat Commun* **2015,** *6*, 6267.

6. Hemphill, J.; Borchardt, E. K.; Brown, K.; Asokan, A.; Deiters, A., Optical Control of CRISPR/Cas9 Gene Editing. *J Am Chem Soc* **2015,** *137* (17), 5642-5.

7. Dowdy, S. F., Overcoming cellular barriers for RNA therapeutics. *Nat Biotechnol* **2017,** *35* (3), 222-229.

8. Mout, R.; Ray, M.; Lee, Y. W.; Scaletti, F.; Rotello, V. M., In Vivo Delivery of CRISPR/Cas9 for Therapeutic Gene Editing: Progress and Challenges. *Bioconjug Chem* **2017,** *28* (4), 880-884.

9. Wang, H. X.; Li, M.; Lee, C. M.; Chakraborty, S.; Kim, H. W.; Bao, G.; Leong, K. W., CRISPR/Cas9-Based Genome Editing for Disease Modeling and Therapy: Challenges and Opportunities for Nonviral Delivery. *Chem Rev* **2017,** *117* (15), 9874-9906.

10. Zuris, J. A.; Thompson, D. B.; Shu, Y.; Guilinger, J. P.; Bessen, J. L.; Hu, J. H.; Maeder, M. L.; Joung, J. K.; Chen, Z. Y.; Liu, D. R., Cationic lipid-mediated delivery of proteins enables efficient protein-based genome editing in vitro and in vivo. *Nat Biotechnol* **2015,** *33* (1), 73-80.

11. Mout, R.; Ray, M.; Yesilbag Tonga, G.; Lee, Y. W.; Tay, T.; Sasaki, K.; Rotello, V. M., Direct Cytosolic Delivery of CRISPR/Cas9-Ribonucleoprotein for Efficient Gene Editing. *ACS Nano* **2017,** *11* (3), 2452-2458.

12. Sun, W.; Ji, W.; Hall, J. M.; Hu, Q.; Wang, C.; Beisel, C. L.; Gu, Z., Self-assembled DNA nanoclews for the efficient delivery of CRISPR-Cas9 for genome editing. *Angew Chem Int Ed Engl* **2015,** *54* (41), 12029-33.

13. Miller, J. B.; Zhang, S.; Kos, P.; Xiong, H.; Zhou, K.; Perelman, S. S.; Zhu, H.; Siegwart, D. J., Non-Viral CRISPR/Cas Gene Editing In Vitro and In Vivo Enabled by Synthetic Nanoparticle Co-Delivery of Cas9 mRNA and sgRNA. *Angew Chem Int Ed Engl* **2017,** *56* (4), 1059-1063.

14. Li, H. E., M.; O'Keeffe, M.; Yaghi, O. M., Design and synthesis of an exceptionally stable and highly porous metal-organic framework *Nature* **1999,** *402* (6759), 276-279.

15. Phan, A.; Doonan, C. J.; Uribe-Romo, F. J.; Knobler, C. B.; O'Keeffe, M.; Yaghi, O. M., Synthesis, structure, and carbon dioxide capture properties of zeolitic imidazolate frameworks. *Acc Chem Res* **2010,** *43* (1), 58-67.

16. Venna, S. R.; Carreon, M. A., Highly permeable zeolite imidazolate framework-8 membranes for CO_2/CH_4 separation. *J Am Chem Soc* **2010,** *132* (1), 76-8.

17. Doonan, C.; Ricco, R.; Liang, K.; Bradshaw, D.; Falcaro, P., Metal-Organic Frameworks at the Biointerface: Synthetic Strategies and Applications. *Accounts Chem Res* **2017,** *50* (6), 1423-1432.

18. Horcajada, P.; Gref, R.; Baati, T.; Allan, P. K.; Maurin, G.; Couvreur, P.; Ferey, G.; Morris, R. E.; Serre, C., Metal-Organic Frameworks in Biomedicine. *Chemical Reviews* **2012,** *112* (2), 1232-1268.

19. Yang, J.; Zhang, Y. B.; Liu, Q.; Trickett, C. A.; Gutierrez-Puebla, E.; Monge, M. A.; Cong, H.; Aldossary, A.; Deng, H.; Yaghi, O. M., Principles of Designing Extra-Large Pore Openings and Cages in Zeolitic Imidazolate Frameworks. *J Am Chem Soc* **2017,** *139* (18), 6448-6455.

20. Adhikari, C.; Das, A.; Chakraborty, A., Zeolitic Imidazole Framework (ZIF) Nanospheres for Easy Encapsulation and Controlled Release of an Anticancer Drug Doxorubicin under Different External Stimuli: A Way toward Smart Drug Delivery System. *Mol Pharm* **2015,** *12* (9), 3158-66.

21. Deng, J.; Wang, K.; Wang, M.; Yu, P.; Mao, L., Mitochondria Targeted Nanoscale Zeolitic Imidazole Framework-90 for ATP Imaging in Live Cells. *J Am Chem Soc* **2017,** *139* (16), 5877-5882.

22. Liang, K.; Ricco, R.; Doherty, C. M.; Styles, M. J.; Bell, S.; Kirby, N.; Mudie, S.; Haylock, D.; Hill, A. J.; Doonan, C. J.; Falcaro, P., Biomimetic mineralization of metal-organic frameworks as protective coatings for biomacromolecules. *Nature Communications* **2015,** *6*.

23. Shieh, F. K.; Wang, S. C.; Yen, C. I.; Wu, C. C.; Dutta, S.; Chou, L. Y.; Morabito, J. V.; Hu, P.; Hsu, M. H.; Wu, K. C. W.; Tsung, C. K., Imparting Functionality to Biocatalysts via Embedding Enzymes into Nanoporous Materials by a de Novo Approach: Size-Selective Sheltering of Catalase in Metal-Organic Framework Microcrystals. *Journal of the American Chemical Society* **2015,** *137* (13), 4276-4279.

24. Mishra, S.; Heidel, J. D.; Webster, P.; Davis, M. E., Imidazole groups on a linear, cyclodextrin-containing polycation produce enhanced gene delivery via multiple processes. *J Control Release* **2006,** *116* (2), 179-91.

25. Li, M.; Tao, Y.; Shu, Y. L.; LaRochelle, J. R.; Steinauer, A.; Thompson, D.; Schepartz, A.; Chen, Z. Y.; Liu, D. R., Discovery and Characterization of a Peptide That Enhances Endosomal Escape of Delivered Proteins in Vitro and in Vivo. *Journal of the American Chemical Society* **2015,** *137* (44), 14084-14093.

TOC Figure